GEOLOGY | THE GEOLOGICAL SOCIETY OF AMERICA®

https://doi.org/10.1130/G51550.1

Manuscript received 11 July 2023
Manuscript accepted 18 July 2023

Published online 4 August 2023

Seismic anisotropy indicates organized melt beneath the Mid-Atlantic Ridge aids seafloor spreading

J.M. Kendall[1,*], D. Schlaphorst[2], C.A. Rychert[3,4], N. Harmon[3,4], M. Agius[5], and S. Tharimena[6]

[1]Department of Earth Sciences, University of Oxford, South Parks Road, OX1 3AN Oxford, UK
[2]Instituto Dom Luiz (IDL), Faculdade de Ciências, Universidade de Lisboa, Campo Grande, 1749-016 Lisbon, Portugal
[3]Ocean and Earth Science, University of Southampton, Southampton SO143ZH, UK
[4]Geology and Geophysics, Woods Hole Oceanographic Institution, Woods Hole, Massachusetts 02543, USA
[5]Department of Geosciences, Faculty of Science, University of Malta, Msida MSD 2080, Malta
[6]Schibsted ASA, Akersgata 55, 0180 Oslo, Norway

ABSTRACT

Lithospheric plates diverge at mid-ocean ridges and asthenospheric mantle material rises in response. The rising material decompresses, which can result in partial melting, potentially impacting the driving forces of the system. Yet the geometry and spatial distribution of the melt as it migrates to the ridge axis are debated. Organized melt fabrics can cause strong seismic anisotropy, which can be diagnostic of melt, although this is typically not found at ridges. We present anisotropic constraints from an array of 39 ocean-bottom seismometers deployed on 0–80 Ma lithosphere from March 2016 to March 2017 near the equatorial Mid-Atlantic Ridge (MAR). Local and SKS measurements show anisotropic fast directions away from the ridge axis, which are consistent with strain and associated fabric caused by plate motions with short delay times, δt (<1.1 s). Near the ridge axis, we find several ridge-parallel fast splitting directions, φ, with SKS δt that are much longer (1.7–3.8 s). This is best explained by ridge-parallel sub-vertical orientations of sheet-like melt pockets. This observation is much different than anisotropic patterns observed at other ridges, which typically reflect fabric related to plate motions. One possibility is that thicker sub-ridge lithosphere with steep sub-ridge topography beneath slower spreading centers focuses melt into vertical, ridge-parallel melt bands, which effectively weakens the plate. Associated buoyancy forces elevate the sub-ridge plate, providing greater potential energy and enhancing the driving forces of the plates.

INTRODUCTION

In the classic passive seafloor-spreading model, oceanic plate motions and the associated plate divergence that occur at mid-ocean ridges are driven by far-field gravitational forces that pull denser, older plates down at subduction zones (Forsyth and Uyeda, 1975). In this model, upwelling corner flow and decompression melting occur passively at ridges in response to plate motions (Forsyth, 1992). This model works particularly well for the Pacific Ocean, which is surrounded by a large system of subduction zones associated with the Ring of Fire. Other factors could play a role, such as gravitational forces acting on the topography at ridges (Forsyth and Uyeda, 1975) or melt buoyancy forces (Parmentier and Morgan, 1990; Katz, 2010; Eilon and Abers, 2017); although these are typically thought to be far less important, particularly in the Pacific. However, a global understanding of partial melt and the driving forces of plate motions has proven challenging, especially since constraints from non-Pacific ridges have been sparse.

Seismic anisotropy is an important diagnostic for understanding mantle flow and partial melt and their relationship to plate motions and their driving forces. Seismic anisotropy refers to the variation in wave speed with propagation direction and/or the polarization of seismic waves. Shear wave anisotropy can be described by the splitting parameters δt (the time delay between the fast and slow shear wave) and φ (the polarization direction of the fast shear wave). In the mantle, plate motions result in shear strains, which cause the anisotropic mineral olivine to align into an organized fabric (Jung and Karato, 2001); whereas, in the shallow crust, oriented cracks can be a more prevalent mechanism (Dunn and Toomey, 2001; Barclay and Toomey, 2003). Alternative mechanisms include compositional fabrics or organized melt (Holtzman and Kendall, 2010; Rychert and Harmon, 2017).

SKS splitting from the fast-spreading East Pacific Rise (EPR) and the intermediate-spreading Juan de Fuca Ridge suggest moderate δt (1–2 s) with φ generally in the direction of plate motion (Wolfe and Solomon, 1998; Harmon et al., 2004; Martin-Short et al., 2015). This is consistent with moderate strain accumulation in the mantle related to plate motion and the passive spreading model. In contrast, the Atlantic Ocean is not surrounded by large subduction-zone trenches, and the forces driving its plate motions are less well understood. Evaluation of the differences between the fast-spreading Pacific and slower spreading ridges like the Mid-Atlantic has proven challenging given that there has been little observational evidence at slow spreading centers.

We present teleseismic SKS and local splitting measurements from an array of 39 ocean-bottom seismometers near the equatorial Mid-Atlantic Ridge (MAR), recorded from March 2016 to March 2017 (see the Supplemental Material[1];

Michael Kendall https://orcid.org/0000-0002-1486-3945
*mike.kendall@earth.ox.ac.uk

[1]Supplemental Material. Additional information about the experiment and the shear-wave splitting analysis and its analyses and interpretation. It includes two supplementary figures showing local S-wave event locations, local S splitting delay times and their uncertainties against event depth, backazimuth, and event-to-station path length. Also included are two tables listing station details, individual and stacked teleseismic SKS results, and individual local S results. Please visit https://doi.org/10.1130/GEOL.S.23713431 to access the supplemental material, and contact editing@geosociety.org with any questions.

CITATION: Kendall, J.M., et al., 2023, Seismic anisotropy indicates organized melt beneath the Mid-Atlantic Ridge aids seafloor spreading: Geology, v. 51, p. 968–972, https://doi.org/10.1130/G51550.1

Wuestefeld et al., 2010). In this region, small-scale upwellings and downwellings have been inferred from seismic velocity anomalies and conductivity anomalies (Wang et al., 2020; Harmon et al., 2021). Steep gradients on the base of the lithosphere are also imaged beneath the ridge axis (Saikia et al., 2021). Comparison with petrophysical predictions suggests that melt may be required in several punctuated anomalies and channel features beneath the plate (Harmon et al., 2021).

RESULTS

We divided our SKS results into two groups. Two-dimensional (2-D) numerical predictions predict $\delta t = 1.0–1.5$ s for slow spreading centers (Blackman and Kendall, 2002). Therefore, we classify our SKS results that that are similar to or less than the predictions ($\delta t = 0.4–1.1$ s) as small and we classify our δt that are longer than predictions ($\delta t = 1.7–3.8$ s) as large.

The majority of the SKS δt measurements are small: 13 out of 19 range from 0.4 s to 1.1 s (Fig. 1). Most of the small SKS δt measurements on the African plate are also associated with φ measurements parallel to the absolute plate motion (APM) direction (~51°), with seven out of 10 measurements within 10° and within error (I14D, L16D, L18D, L21D, S22D, L30A, and S38D in Fig. 1). These observations of small δt with φ in the APM direction are all distant from the ridge axis. There is also one small δt on the North American plate with φ within 5° of the spreading direction, ~80° azimuth (I34D). There are five small δt (0.6–1.1 s) that do not correspond to the spreading direction or the APM direction of Africa (S03D, S06D, I12D, S26D, I28D). A complete list of φ, δt, and error bars is provided in the Supplemental Material.

There are six SKS results with large δt (>1.7 s): four have φ parallel to the ridge (~170° azimuth) within error. The large, ridge-parallel δt are all within 80 km of the ridge axis and on seafloor that is younger than 21 Ma (Fig. 2). The two ridge-parallel φ near the ridge in the north have the largest δt (3.6–3.8 s) in comparison to the others (1.7–2.7 s). One of the large ridge-parallel results is not on a ridge or next to it, rather it is across the transform to the south. Two of the large δt are nearly perpendicular to the ridge (S11D and S29D).

S-wave splitting in local events shows a mix of directions in φ (Fig. 3) and δt with average values of 0.2 s. Near the northern ridge axis, φ directions are mainly ridge-parallel (R1 in Fig. 3). Eastward from the northern ridge segment, the predominant φ direction is roughly southwest-northeast (R2 to R5 in Fig. 3). Near the southern ridge axis, R9 shows a mix of φ, although it shows a ridge-sub-parallel φ on average. West of the southern ridge, two groupings show a φ more consistent with the spreading direction (R8 and R6), and one shows a dominant φ between the ridge strike and spreading direction (R7).

DISCUSSION AND IMPLICATIONS

The SKS splitting results away from the ridge segments on the African plate (I14D, L16D, L18D, L21D, S22D, L30A, S38D in Fig. 1), are best interpreted in terms of strain-induced alignment of olivine with A-type fabric (Jung and Karato, 2001). The φ directions, which are primarily within 10° of APM, are suggestive of strain related to the motion of the tectonic plate

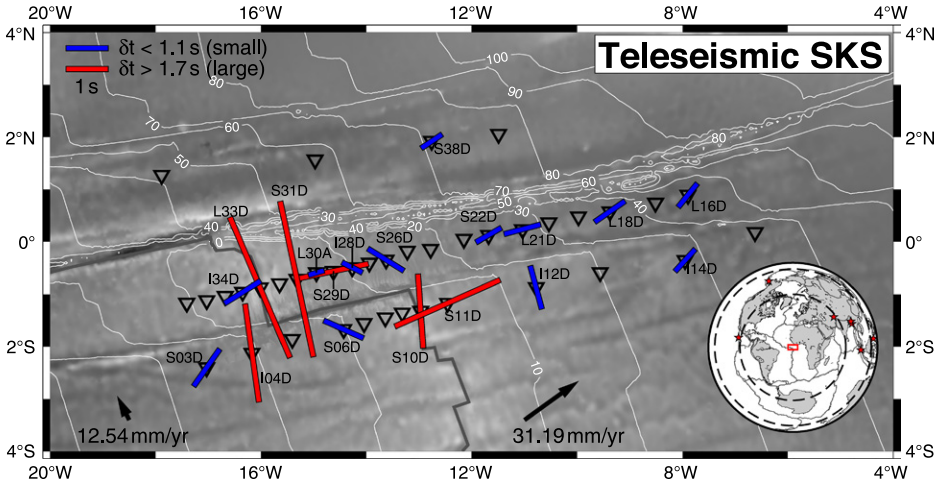

Figure 1. Map of Passive Imaging of the Lithosphere Asthenosphere Boundary (PILAB) project (https://www.southampton.ac.uk/oes/research/projects/passive-imaging-of-the-lithosphere-asthenosphere-boundary.page) stations and SKS splitting results. Inverted black triangles are ocean-bottom seismometer (OBS) stations; white contours are plate ages in Ma; plate boundaries are gray lines; blue bars show SKS splitting for small delay times (δt <1.1 s) and red bars show large δt (>1.7 s); black arrows show absolute plate motions (APM) (Gripp and Gordon, 1990); red box in the inset shows the study area; red stars in the inset indicate teleseismic events within the distance criteria (black dashed circles). Background shows bathymetry (Becker et al., 2009; Harmon et al., 2018).

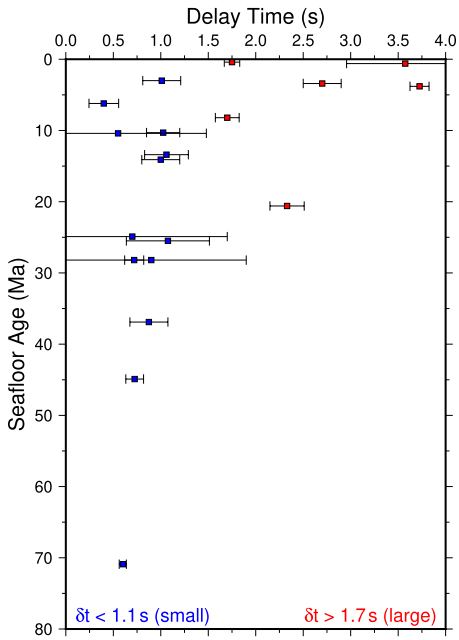

Figure 2. SKS splitting delay time, δt, verses plate age. Note that the largest splitting values are observed on young plate regions.

over the underlying mantle. A 50–60-km-thick layer of 5–8% anisotropy can explain the SKS observations of $\delta t = 0.4–1.1$ s. This is consistent with previous estimates from local surface-wave tomography of the magnitude of anisotropy (up to 5%) and also the thickness of the lithosphere-asthenosphere system (50–60 km; Saikia et al., 2021). It is slightly larger than the 1.7–4% anisotropy inferred from constraints on older Atlantic seafloor to the west (Gaherty et al., 2004; Russell and Gaherty, 2021), potentially because of variations in dynamics with time. The small δt (0.4–1.1 s) are similar or smaller than 2-D numerical predictions for slow spreading ($\delta t = 1.0–1.5$ s) (Blackman and Kendall, 2002). Smaller δt may be caused by complex, less-organized, 3-D mantle flow, which is supported by shear velocity and resistivity anomalies (Harmon et al., 2021).

Our off-axis SKS measurements resemble observations from the ultrafast EPR at 17 °S and the intermediate Juan de Fuca Ridge in Cascadia. Our small δt (0.4–1.1 s; blue symbols in Figs. 1 and 2) are similar to those observed at the EPR and most measurements from Cascadia that are away from the trench ($\delta t < 2$ s) (Wolfe and Solomon, 1998; Harmon et al., 2004; Martin-Short et al., 2015). Our near-APM φ values at I14D, L16D, L18D, L21D, S22D, L30A, and S38D are similar to the approximately APM or spreading direction observations at the EPR and Cascadia (see the Supplemental Material).

The local splitting results likely reflect a combination of crustal and mantle processes. Focusing on the rose diagrams in Figure 2, near the ridge (R1 and R9) the dominantly ridge-parallel or sub-ridge-parallel φ values likely reflect crack-induced anisotropy. The local δt

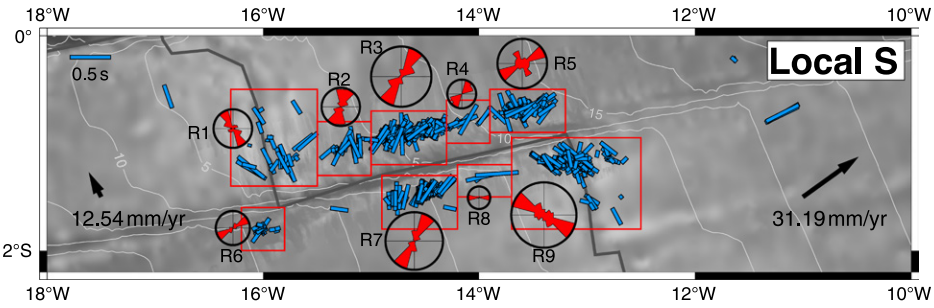

Figure 3. Map of local event shear wave splitting results (blue bars) plotted at the event-station midpoints. Rose diagrams indicate polarization direction of the fast shear wave (φ) weighted by delay time (δt) for the bins (red boxes). Absolute plate motions are shown with black arrows.

values (0.2 s on average, but as high as 0.6 s in some cases) are larger than the ~0.1 s predicted for shallow crustal cracking anisotropy reported at other spreading centers (Dunn and Toomey, 2001; Barclay and Toomey, 2003). Therefore, crack density may be larger or extend to greater depths. Alternatively, the rose diagram results may reflect some degree of mantle anisotropy. These rose diagrams are dominated by the deepest events (30–40 km) since they have larger δt (and larger weighting) (Schlaphorst et al., 2023). Away from the ridge axis (R2–R5 and R7–R9), φ directions are also generally consistent with the rotation of stresses in the mantle predicted by numerical modeling of oceanic transforms (Morgan and Parmentier, 1984), suggesting that crustal cracking near the ridge heals at older ages (see the Supplemental Material).

The large SKS δt (1.7–3.8 s) near the ridge axis at stations L33D, S31D, S29D, S10D, and S11D are not easily explained by subsolidus conditions. Numerical modeling suggests near-ridge anisotropy from A-type olivine would result in $\delta t < 1.5$ s (Blackman and Kendall, 2002), in predominantly ridge-perpendicular directions. Vertical upwelling, ridge-parallel flow, and water-rich E-type fabrics (Jung and Karato, 2001) can cause mineralogical alignment of olivine and ridge-parallel φ, although with δt that are insufficient to describe our observations (see the Supplemental Material). Crustal cracking in the shallow crust can similarly result in ridge-parallel φ, although this is also expected to be smaller than the large observed δt (see the Supplemental Material). A compositional fabric can produce ridge-parallel φ, although again this cannot explain the large δt (see the Supplemental Material).

Alternatively, the contrast between the slow seismic velocities of partial melt in comparison to the faster solid mantle can easily explain the large δt (>1.7 s). Many scenarios and melt geometries are possible. However, as an example, a model with 2% partial melt in disc-shaped melt inclusions (Tandon and Weng, 1984) with high wetting angles (Takei, 2005), vertically dipping and aligned in the ridge strike direction over a 30-km-thick region can explain the observed φ and δt. Two-percent partial melt is also consistent with that inferred in near-ridge mantle anomalies from Rayleigh wave tomography and magnetotelluric imaging (Harmon et al., 2021). Larger δt near the northern ridge segment in comparison to the southern ridge segment is consistent with higher percentages of partial melt in the mantle, and also with the sub-ridge crust inferred from seismic and magnetotelluric imaging, tidal triggering, and residual Mantle Bouguer Anomalies (Harmon et al., 2018; Harmon et al., 2021; Leptokaropoulos et al., 2021). The two strong splitting results near the ridge axis with ridge-perpendicular trends (S29D and S11D) are intriguing; however, further investigation is required, and they are not central to our conclusions (see the Supplemental Material). This is similarly true for the few SKS measurements with small δt with φ that do not follow the APM trend or predicted stress rotations (S06D, I12D, S26D, I28D) (see the Supplemental Material).

Our large δt with ridge-parallel φ near the ridge axis are much different than observations from other ridges, where APM or spreading-parallel directions are observed across the ridge axes. Alignment that resembles nearby APM or plate spreading is observed at the EPR and Cascadia (Wolfe and Solomon, 1998; Harmon et al., 2004; Martin-Short et al., 2015). The one exception is the location of the Axial Seamount on the Juan de Fuca Ridge, where ridge-parallel alignment with $\delta t = 1$ s is observed (Martin-Short et al., 2015). Overall, this suggests a different style of upwelling and deep magma emplacement at the MAR in comparison to other ridges away from hotspots.

The difference between our results and those from faster spreading centers may be facilitated by differences in the sub-ridge structures. High advection rates at faster spreading centers result in minimal lateral conductive cooling effects, near-zero sub-ridge plate thicknesses, and plates that thicken gradually with age, and this is observed at the EPR (Fig. 4; Harmon et al.,

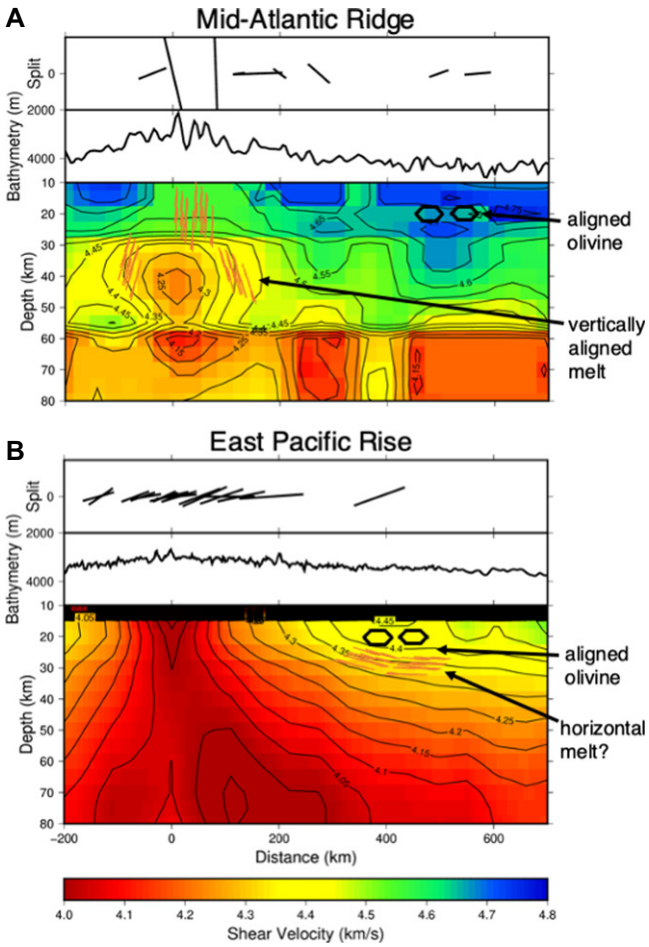

Figure 4. Atlantic-Pacific comparison. (A) SKS splitting directions relative to the ridge axis and strengths (proportional to length) from the slow-spreading Mid-Atlantic Ridge (black bars) above shear wave velocities from surface waves (Saikia et al., 2021). (B) The same as in A, but at the fast-spreading East Pacific Rise (Harmon et al., 2009). Thin orange lines indicate inferred organized melt. Black symbols show inferred olivine alignment.

2009). Melt flow is predicted to occur more horizontally (Sim et al., 2020; Katz et al., 2022), and this would not necessarily cause any strong azimuthal anisotropy (Holtzman and Kendall, 2010). Melt extraction at fast spreading centers may also be more efficient, at least in part because of the negligible thickness of the subridge plate.

In contrast, greater degrees of lateral conductive cooling at slower spreading centers such as the MAR result in non-negligible subridge plate thicknesses (Parmentier and Morgan, 1990; Saikia et al., 2021). The thickness of the lithosphere increases rapidly over a short distance, creating a sub-vertical lithosphere base, or permeability boundary, that channels melt toward the ridge (Holtzman and Kendall, 2010). Dike emplacement may also occur in the lithosphere (Havlin et al., 2013; Pec et al., 2015). If melt is present at the percentages predicted by seismic imaging (∼2%; Harmon et al., 2021), our splitting result suggests that the melt extends over at least 30 km in depth. Subvertical melt alignment along the base of the plate is supported by our shear wave velocities from surface waves that suggest a relatively steep gradient on the base of the plate near the ridge axis that extends to ∼60 km depth (Saikia et al., 2021).

The interaction of the partial melt with the non-negligible plate beneath the ridge may play a larger role in driving plate tectonics at slow spreading centers. An ∼2% melt beneath the northern ridge segment would result in an additional buoyancy pressure of 9 MPa, assuming a 30-km-deep column and a density reduction of ∼30 kg/m^3 from the combined effects of lower-density melt. This amount of melt buoyancy accounts for approximately 25% of the expected pressure from ridge push for the height of the MAR in this region, in comparison to the ∼5-km-deep surrounding seafloor, for a purely thermal model (see the Supplemental Material). This additional buoyancy may also explain the shallower ridge bathymetries in the Atlantic in comparison to the Pacific, 2.4–2.5 km versus 2.7–2.8 km, respectively (Crosby and McKenzie, 2009), which would also be associated with greater associated potential energy. Therefore, our result suggests that the non-negligible plate thickness at slow spreading center axes, like the Atlantic, focuses melt and facilitates its organization beneath the ridge. Furthermore, ridge-parallel oriented melt will weaken the plate boundary, focusing strain at the ridge (Buck et al., 2005). In addition, melt buoyancy forces elevate the non-negligible subridge plate, which aids the driving forces of plate tectonics at slow spreading centers. Cumulatively, our observations suggest that ridge forces at slow spreading centers could play a more significant role in driving plate motions than previously assumed.

ACKNOWLEDGMENTS

C. Rychert and N. Harmon acknowledge funding from the Natural Environment Research Council (NERC) (grant NE/M003507/1) and the European Research Council (grant GA 638665). C. Rychert acknowledges funding from the National Science Foundation (grants EAR-2147918 and OCE-231613). J. Kendall was funded by NERC grant NE/M004643/1. We thank the captains and crews of R/V *Marcus G. Langseth* (cruise MGL2016–02) and RRS *Discovery* (cruise DY072), and their scientific technicians. D. Schlaphorst acknowledges financial support from the Fundação para a Ciência e a Tecnologia (FCT) through project UIDB/50019/2020–IDL.

REFERENCES CITED

Barclay, A.H., and Toomey, D.R., 2003, Shear wave splitting and crustal anisotropy at the Mid-Atlantic Ridge, 35°N: Journal of Geophysical Research: Solid Earth, v. 108, B8, https://doi.org/10.1029/2001JB000918.

Becker, J.J., et al., 2009, Global bathymetry and elevation data at 30 arc seconds resolution: SRTM30_PLUS: Marine Geodesy, v. 32, no. 4, p. 355–371, https://doi.org/10.1080/01490410903297766.

Blackman, D.K., and Kendall, J.M., 2002, Seismic anisotropy in the upper mantle; 2. Predictions for current plate boundary flow models: Geochemistry, Geophysics, Geosystems, v. 3, no. 9, https://doi.org/10.1029/2001gc000247.

Buck, W.R., Lavier, L.L., and Poliakov, A.N.B., 2005, Modes of faulting at mid-ocean ridges: Nature, v. 434, p. 719–723, https://doi.org/10.1038/nature03358.

Crosby, A.G., and McKenzie, D., 2009, An analysis of young ocean depth, gravity and global residual topography: Geophysical Journal International, v. 178, no. 3, p. 1198–1219, https://doi.org/10.1111/j.1365-246X.2009.04224.x.

Dunn, R.A., and Toomey, D.R., 2001, Crack-induced seismic anisotropy in the oceanic crust across the East Pacific Rise (9°30′N): Earth and Planetary Science Letters, v. 189, no. 1–2, p. 9–17, https://doi.org/10.1016/S0012-821X(01)00353-3.

Eilon, Z.C., and Abers, G.A., 2017, High seismic attenuation at a mid-ocean ridge reveals the distribution of deep melt: Science Advances, v. 3, https://doi.org/10.1126/sciadv.1602829.

Forsyth, D., and Uyeda, S., 1975, On the relative importance of the driving forces of plate motion: Geophysical Journal International, v. 43, no. 1, p. 163–200, https://doi.org/10.1111/j.1365-246X.1975.tb00631.x.

Forsyth, D.W., 1992, Geophysical constraints on mantle flow and melt generation beneath midocean ridges, *in* Morgan, J.P., Blackman, D.K., and Sinton, J.M., eds., Mantle Flow and Melt Generation at Mid-Ocean Ridges: American Geophysical Union, Geophysical Monograph Series v. 71, p. 1–65, https://doi.org/10.1029/GM071p0001.

Gaherty, J.B., Lizarralde, D., Collins, J.A., Hirth, G., and Kim, S., 2004, Mantle deformation during slow seafloor spreading constrained by observations of seismic anisotropy in the western Atlantic: Earth and Planetary Science Letters, v. 228, no. 3–4, p. 255–265, https://doi.org/10.1016/j.epsl.2004.10.026.

Gripp, A.E., and Gordon, R.G., 1990, Current plate velocities relative to the hotspots incorporating the NUVEL-1 global plate motion model: Geophysical Research Letters, v. 17, no. 8, p. 1109–1112, https://doi.org/10.1029/GL017i008p01109.

Harmon, N., Forsyth, D.W., Fischer, K.M., and Webb, S.C., 2004, Variations in shear-wave splitting in young Pacific seafloor: Geophysical Research Letters, v. 31, no. 15, https://doi.org/10.1029/2004GL020495.

Harmon, N., Forsyth, D.W., and Weeraratne, D.S., 2009, Thickening of young Pacific lithosphere from high-resolution Rayleigh wave tomography: A test of the conductive cooling model: Earth and Planetary Science Letters, v. 278, no. 1–2, p. 96–106, https://doi.org/10.1016/j.epsl.2008.11.025.

Harmon, N., Rychert, C.A., Agius, M.R., Tharimena, S., Le Bas, T.P., Kendall, J.M., and Constable, S., 2018, Marine geophysical investigation of the Chain Fracture Zone in the equatorial Atlantic from the PI-LAB Experiment: Journal of Geophysical Research: Solid Earth, v. 123, p. 11,016–11,030, https://doi.org/10.1029/2018JB015982.

Harmon, N., Wang, S., Rychert, C.A., Constable, S., and Kendall, J.M., 2021, Shear velocity inversion guided by resistivity structure from the PI-LAB Experiment for integrated estimates of partial melt in the mantle: Journal of Geophysical Research: Solid Earth, v. 126, no. 8, https://doi.org/10.1029/2021JB022202.

Havlin, C., Parmentier, E.M., and Hirth, G., 2013, Dike propagation driven by melt accumulation at the lithosphere–asthenosphere boundary: Earth and Planetary Science Letters, v. 376, p. 20–28, https://doi.org/10.1016/j.epsl.2013.06.010.

Holtzman, B.K., and Kendall, J.M., 2010, Organized melt, seismic anisotropy, and plate boundary lubrication: Geochemistry, Geophysics, Geosystems, v. 11, https://doi.org/10.1029/2010GC003296.

Jung, H., and Karato, S.-I., 2001, Water-induced fabric transitions in olivine: Science, v. 293, p. 1460–1463, https://doi.org/10.1126/science.1062235.

Katz, R., 2010, Porosity-driven convection and asymmetry beneath mid-ocean ridges: Geochemistry, Geophysics, Geosystems, v. 11, https://doi.org/10.1029/2010GC003282.

Katz, R.F., Jones, D.W.R., Rudge, J.F., and Keller, T., 2022, Physics of melt extraction from the mantle: Speed and style: Annual Review of Earth and Planetary Sciences, v. 50, p. 507–540, https://doi.org/10.1146/annurev-earth-032320-083704.

Leptokaropoulos, K., Harmon, N., Hicks, S., Rychert, C., Schlaphorst, D., and Kendall, J., 2021, Tidal triggering of microseismicity at the Equatorial Mid-Atlantic Ridge, inferred from the PI-LAB Experiment: Journal of Geophysical Research: Solid Earth, https://doi.org/10.1029/2021JB022251.

Martin-Short, R., Allen, R.M., Bastow, I.D., Totten, E., and Richards, M.A., 2015, Mantle flow geometry from ridge to trench beneath the Gorda-Juan de Fuca plate system: Nature Geoscience, v. 8, no. 12, p. 965–968, https://doi.org/10.1038/ngeo2569.

Morgan, J.P., and Parmentier, E.M., 1984, Lithospheric stress near a ridge-transform intersection: Geophysical Research Letters, v. 11, no. 2, p. 113–116, https://doi.org/10.1029/GL011i002p00113.

Parmentier, E.M., and Morgan, J.P., 1990, Spreading rate dependence of 3-dimensional structure in oceanic spreading centers: Nature, v. 348, p. 325–328, https://doi.org/10.1038/348325a0.

Pec, M., Holtzman, B. K., Zimmerman, M., and Kohlstedt, D. L., 2016, Reaction infiltration instabilities in experiments on partially molten mantle rocks: Geology, v. 43, no. 7, p. 575–578, https://doi.org/10.1130/G36611.1.

Russell, J.B., and Gaherty, J.B., 2021, Lithosphere structure and seismic anisotropy offshore eastern North America: Implications for continental breakup and ultra-slow spreading dynamics: Journal of Geophysical Research: Solid Earth, v. 126, no. 12, https://doi.org/10.1029/2021JB022955.

Rychert, C.A., and Harmon, N., 2017, Constraints on the anisotropic contributions to velocity discontinuities at ∼60 km depth beneath the Pacific:

Geochemistry, Geophysics, Geosystems, v. 18, https://doi.org/10.1002/2017GC006850.
Saikia, U., Rychert, C.A., Harmon, N., and Kendall, J.M., 2021, Upper mantle anisotropic shear velocity structure at the equatorial Mid-Atlantic Ridge constrained by Rayleigh wave group velocity analysis from the PI-LAB experiment: Geochemistry, Geophysics, Geosystems, v. 22, no. 3, https://doi.org/10.1029/2020GC009495.
Schlaphorst, D., Rychert, C.A., Harmon, N., Hicks, S.P., Bogiatzis, P., Kendall, J.-M., and Abercrombie, R.E., 2023, Local seismicity around the Chain Transform Fault at the Mid-Atlantic Ridge from OBS observations: Geophysical Journal International, v. 234, no. 2, p. 1111–1124, https://doi.org/10.1093/gji/ggad124.
Sim, S.J., Spiegelman, M., Stegman, D.R., and Wilson, C., 2020, The influence of spreading rate and permeability on melt focusing beneath mid-ocean ridges: Physics of the Earth and Planetary Interiors, v. 304, https://doi.org/10.1016/j.pepi.2020.106486.
Takei, Y., 2005, Deformation-induced grain boundary wetting and its effects on the acoustic and rheological properties of partially molten rock analogue: Journal of Geophysical Research: Solid Earth, v. 110, B12, https://doi.org/10.1029/2005JB003801.
Tandon, G.P., and Weng, G.J., 1984, The effect of aspect ratio of inclusions on the elastic properties of unidirectionally aligned composites: Polymer Composites, v. 5, no. 4, p. 327–333, https://doi.org/10.1002/pc.750050413.
Wang, S., Constable, S., Rychert, C., and Harmon, N., 2020, A lithosphere-asthenosphere boundary and partial melt estimated using marine magnetotelluric data at the central Middle Atlantic Ridge: Geochemistry, Geophysics, Geosystems, v. 21, no. 9, https://doi.org/10.1029/2020GC009177.
Wolfe, C.J., and Solomon, S.C., 1998, Shear-wave splitting and implications for mantle flow beneath the MELT region of the East Pacific Rise: Science, v. 280, p. 1230–1232, https://doi.org/10.1126/science.280.5367.1230.
Wuestefeld, A., Al-Harrasi, O., Verdon, J.P., Wookey, J., and Kendall, J.M., 2010, A strategy for automated analysis of passive microseismic data to image seismic anisotropy and fracture characteristics: Geophysical Prospecting, v. 58, no. 5, p. 755–773, https://doi.org/10.1111/j.1365-2478.2010.00891.x.

Printed in the USA